DAΦNE TECHNICAL NOTE
INFN - LNF, Accelerator Division

Frascati, January 18, 2006
Note: **G-65**

DYNAMIC APERTURE OF THE STRONG RF FOCUSING STORAGE RING

E. Levichev, P. Piminov

Budker Institute of Nuclear Physics, Novosibirsk 630090, Russia

C. Biscari, M. Zobov

Laboratori Nazionali di Frascati, INFN, Frascati, C.P. 13, 00044, Italy

Abstract

Recently a strong RF focusing regime has been proposed as a basic principle for the design of a super factory at the Φ energy. To prove this regime the bunch modulation experiment was proposed at the DAΦNE storage ring. In the paper we present the results of the 6D nonlinear beam dynamics simulation for one of the possible setups of the experiment.

1 INTRODUCTION

Recently the strong RF focusing regime (SRFF) [1] has been proposed at Frascati as a basic principle for the design of an extremely high luminosity electron-positron collider at the Φ en-ergy. This regime is based on the significantly increased amplitude of RF voltage and the high momentum compaction lattice which together produce a bunch length modulation along the ring in such a way to get the minimum bunch length at the interaction point reducing an hour-glass effect and enhancing luminosity.

To examine the new regime a proof-of-principle experiment is proposed now in the existing DAΦNE storage ring [2]. Testing the bunch modulation requires (a) lattice flexibility to control the dispersion function and (b) powerful RF system. First is available in some reasonable range in present DAΦNE due to the independent quadrupoles power supplies, while planning instal-lation of a Tesla type super conducting RF cavity at 1.3 GHz, with a maximum voltage of 10 MV, provides the necessary voltage derivative.

However, strong RF focusing regime intrinsically produces strong coupling of the transverse and longitudinal modes of incoherent oscillations of particle and may deteriorate a stable motion area (dynamic aperture). When the synchrotron tune is high enough, synchrobetatron satellites are not located close to the main resonance lines but form dense resonance net reducing safe tune “islands” size where the dynamic aperture is large.

To study the dynamic aperture of the DAΦNE with SRFF, a simulation of the nonlinear beam dynamics was performed applying the computer code *Acceleraticum* [3], which tracks particles in a 6D manner with the realistic path lengthening in all magnetic elements (it's important for correct simulation of the coupled synchrobetatron motion). Acceleraticum performs synchrobetatron tracking with the help of formalism described in [4] for the following set of variables:

$$\left(x, p_x, z, p_z, \sigma(s) = s - c \cdot t(s), \delta = \frac{E - E_0}{E_0} \right).$$

Transformation of the longitudinal coordinate through the lattice elements is given by the following equation

$$\sigma' = d\sigma / ds = 1 - \left[\left(1 + h(s)x\right)^2 + x'^2 + y'^2 \right]^{1/2},$$

which was solved for many types of elements. Obtained explicit expressions are used in the computer code providing rather fast and effective 6D tracking.

2 LATTICE MODEL

Each DAΦNE ring is composed of four arcs, and two interaction regions shared with the other ring. The new RF system can be installed in one of the interaction regions, so that it can be used by both rings, together or independently. The functio

$$R(s) = \int \frac{D(s')}{\rho(s')} ds' \qquad (1)$$

responsible for the bunch length modulation can be tuned by modifying the dispersion in the dipoles. The regime of strong RF focusing – high momentum compaction factor and high Q_s corresponds to equal contributions to the integral (1) from the four arcs. This regime is referred in [2] as "structure A" and just this lattice is considered in what follows.

The main parameters of the "structure A" are listed in Table 1, the lattice functions are given in Fig.1 [2].

Three lines with chromaticity values in Table 1 mean: natural chromaticity without wiggler nonlinearities, natural chromaticity with wiggler nonlinearities but without the chromatic sextupoles (sext OFF) and chromaticity compensated by sextupole magnets (sext ON). Note that (i) the wigglers contribute significantly to the total chromaticity of the ring and (ii) no reasonable solution for both planes chromaticity compensation was found so the residue vertical chromaticity value is –10.79.

Table 1: Main parameters of the SRRF DAΦNE-A structure.

Q_x/Q_z	4.824/5.212
Q_s at U_{RF} = 5 MV	0.2406
α at IP	0.0727
ξ_{x0}/ξ_{z0}	–6.27/–13.53
ξ_x/ξ_z sext OFF	3.58/–17.43
ξ_x/ξ_z sext ON	0.36/–10.79
ε_x	6.37×10^{-7} m-rad
σ_E/E	3.82×10^{-4}

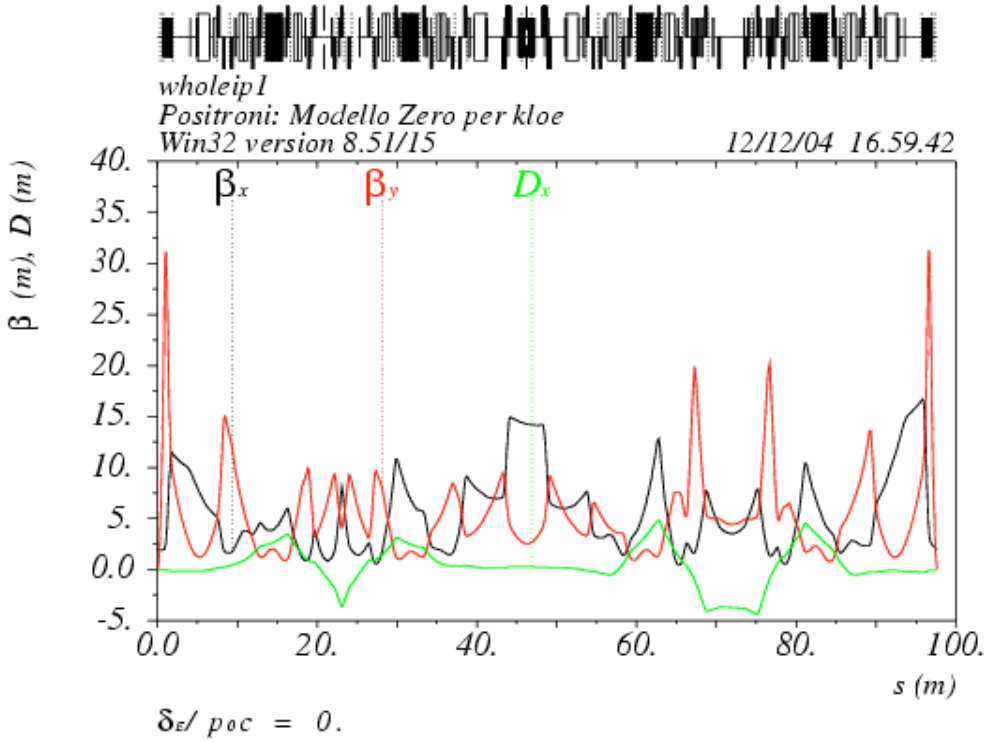

Figure 1: SRRF DAΦNE-A lattice functions.

Figure 2 shows the behavior of the dispersion function for on- and off-momentum particle obtained by tracking and hence depending completely on the momentum deviation $\delta = \Delta p / p_0$:

$$D(\delta) = D_0 + D_1\delta + D_2\delta^2 + \ldots$$

Zero order of the dispersion D_0 almost vanishes in the cavity together with its slope but appears for $\delta = 0$, and this fact can cause additional synchrobetatron resonances.

Figure 3 demonstrates the compaction factor as a function of azimuth along the ring. Four short comb-like sections correspond to the wigglers position.

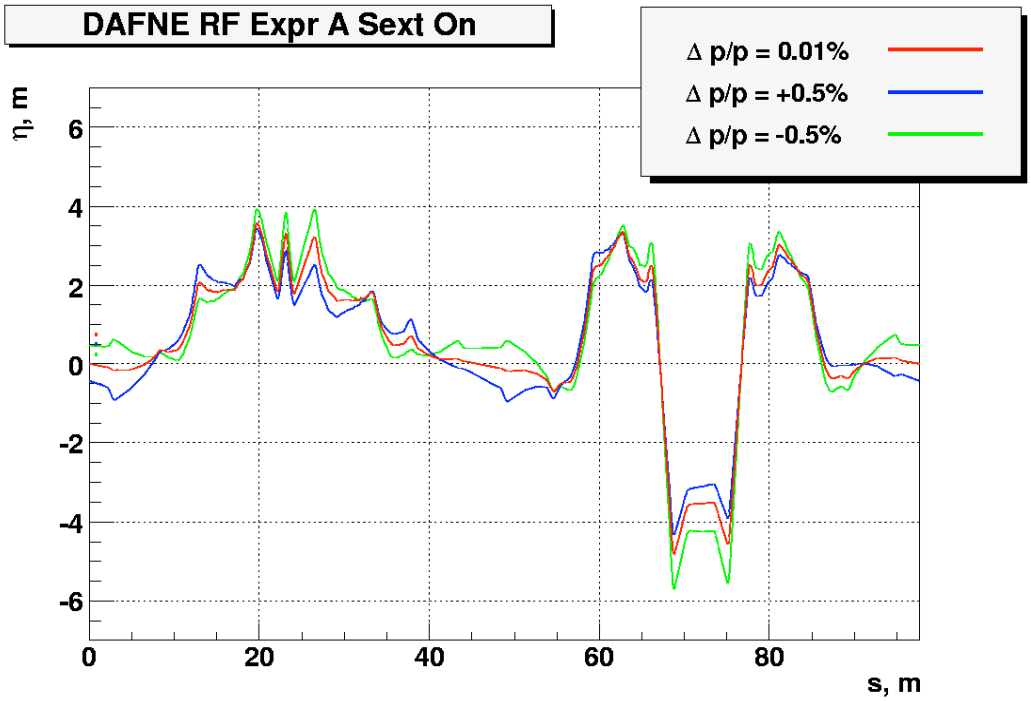

Figure 2: On- and off-momentum dispersion function.

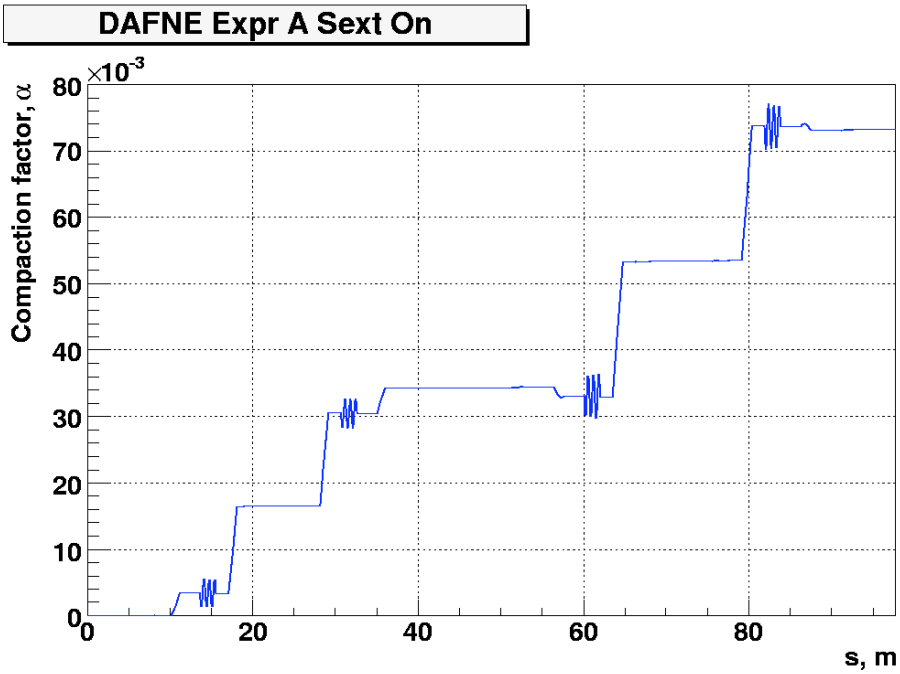

Figure 3: Compaction factor.

In Fig. 4 the bunch length plot is shown for three levels of the RF voltage amplitude. The beginning of the plot corresponds to the interaction point and the minimum of the bunch length. This plot is obtained by tracking of the 6D equilibrium Gaussian distribution (1000 particles) for 1000 revolutions. Such tracking takes into account possible distortion of the particles distribution by nonlinear effects.

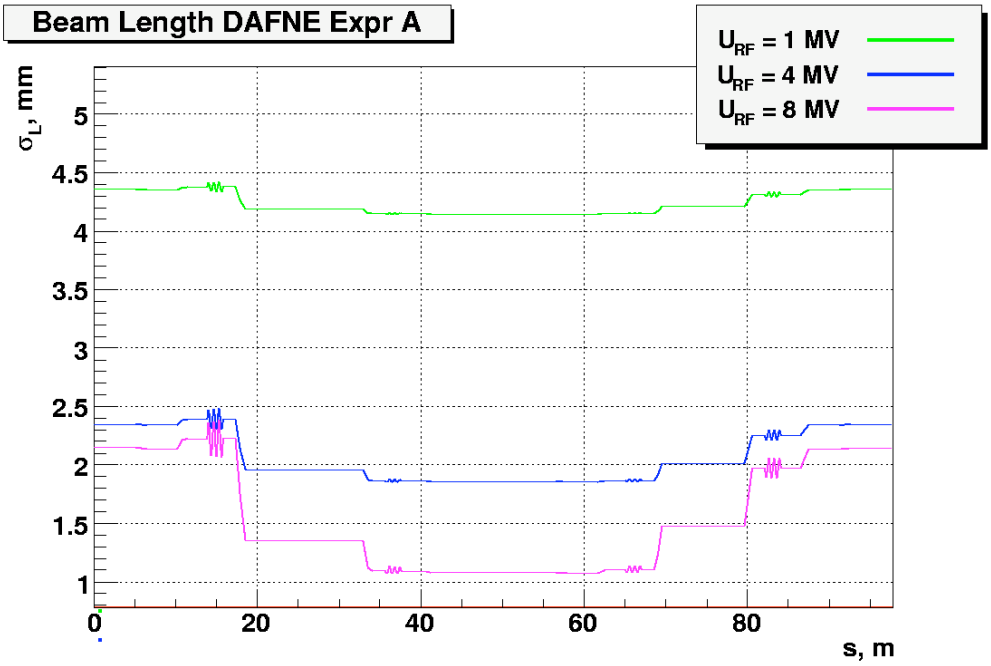

Figure 4: SRRF bunch length modulation for different RF amplitudes.

3 ON-ENERGY DYNAMIC APERTURE

On-energy dynamic aperture is defined by a combined effect of the strong chromatic sextupoles and the wiggler nonlinearities (Fig. 5).

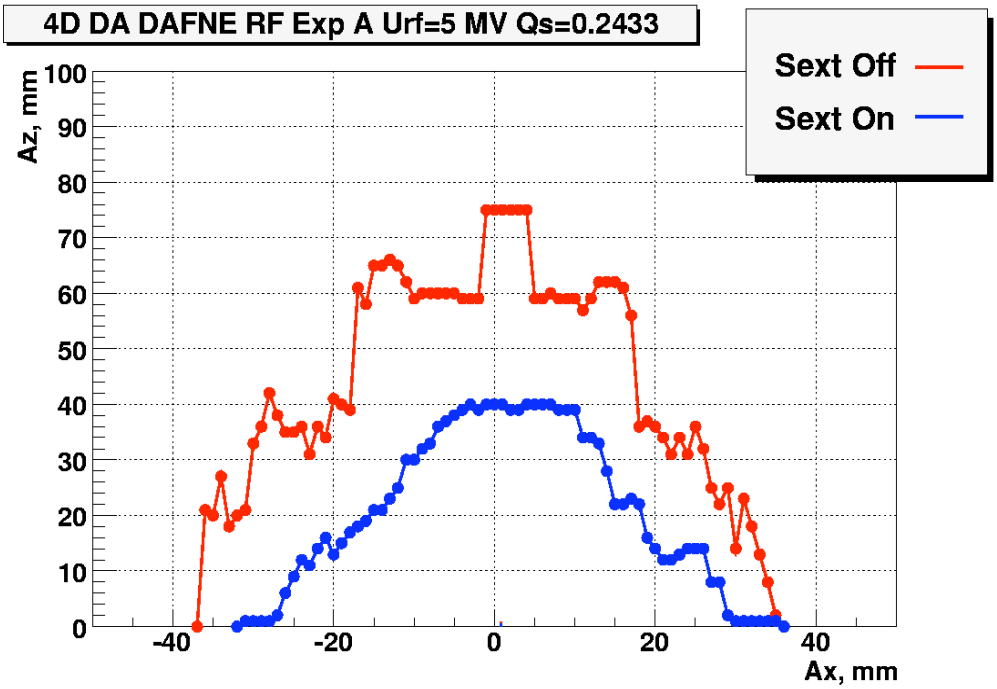

Figure 5: Dynamic aperture due to the wigglers (Sext. Off) and due to both wiggler and sextupole nonlinearity ($\sigma_{x0} = 1.6\text{mm}$, $\sigma_{z0} = 0.27\,\text{mm}$).

The values of the main sextupole resonances harmonics defined as

$$A_{1n} = \frac{1}{48\pi}\sum_m \beta_{xm}^{3/2}(k_2 l)_m \begin{matrix}\cos\\ \sin\end{matrix}(\psi_x - Q_x\theta + n\theta)_m, \qquad (2)$$

$$A_{3n} = \frac{1}{48\pi}\sum_m \beta_{xm}^{3/2}(k_2 l)_m \begin{matrix}\cos\\ \sin\end{matrix}(3\psi_x - 3Q_x\theta + n\theta)_m,$$

$$B_{1n} = \frac{1}{48\pi}\sum_m \beta_{xm}^{1/2}\beta_{ym}(k_2 l)_m \begin{matrix}\cos\\ \sin\end{matrix}(\psi_x - \nu\theta + n\theta)_m,$$

$$B_{\pm n} = \frac{1}{48\pi}\sum_m \beta_{xm}^{1/2}\beta_{ym}(k_2 l)_m \begin{matrix}\cos\\ \sin\end{matrix}(\psi_\pm - \nu_\pm\theta + n\theta)_m,$$

$$\delta = m_x Q_x + m_z Q_z - n$$

$$C_{nm} = \sqrt{Cos^2 + Sin^2}\,/\delta$$

provide information on the most dangerous resonances in the vicinity of the working point, which as it is seen from Table 2 are the coupled resonances (see also the betatron tune scan in Fig. 6).

Table 2: Main resonances strength.

	Cos	*Sin*	δ	C_{nm}
Horizontal harmonics				
A_{15} ($m^{-1/2}$)	–0.08	–0.17	$Q_x - 5 = -0.176$	–1.11
A_{314} ($m^{-1/2}$)	0.28	–0.15	$3Q_x - 14 = 0.473$	0.68
Coupled harmonics				
B_{15} ($m^{-1/2}$)	0.27	–0.37	$Q_x - 5 = -0.176$	**–2.60**
B_{+15} ($m^{-1/2}$)	0.72	0.20	$Q_x + 2Q_z - 15 = 0.248$	**3.01**
$B_{-\,-6}$ ($m^{-1/2}$)	0.65	–0.23	$Q_x - 2Q_z + 6 = 0.401$	1.72

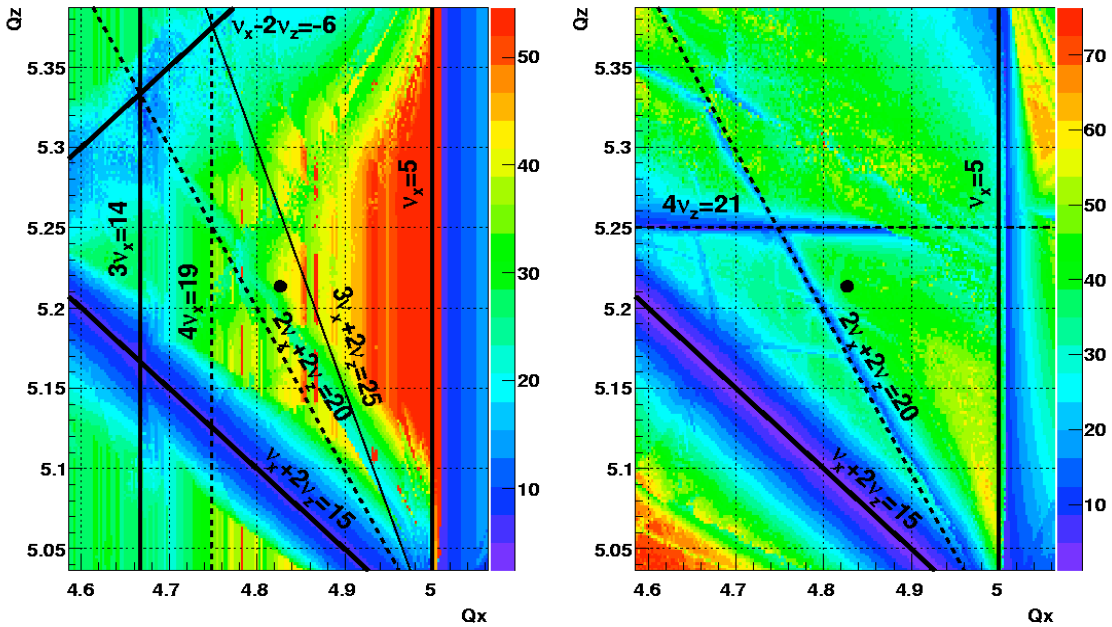

Figure 6: On-energy dynamic aperture (mm) scans. Black point indicates the working tunes.

However, these powerful low order resonances do not limit the dynamic aperture directly, because the tune point is chosen rather far from all of them, but they influence the particle stable area through the secondary resonances which overlap and produce stochastic area. This fact is illustrated in Fig. 7 where many resonance islands are clearly seen at the phase space portrait.

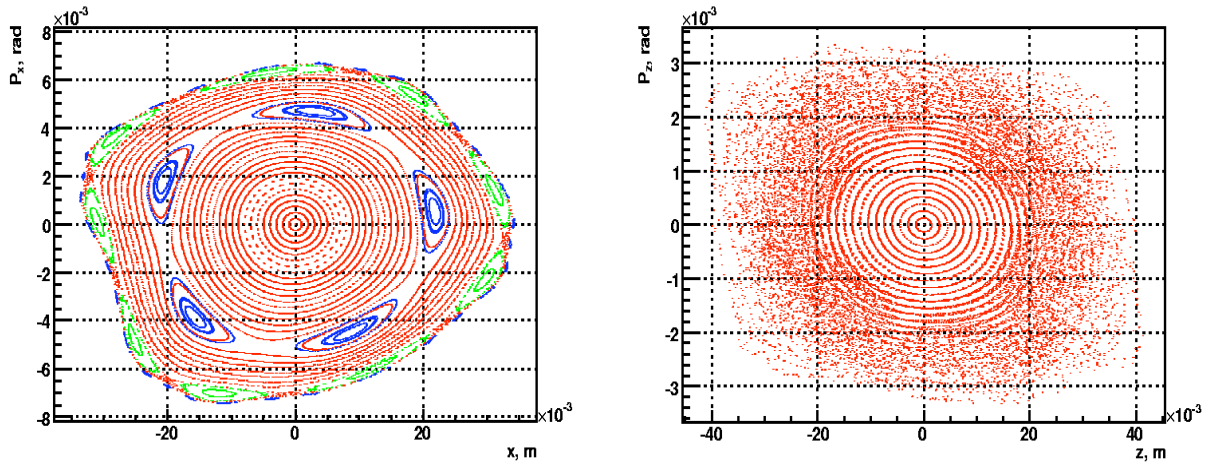

Figure 7: Phase space trajectories. The beta functions in the observation point are $\beta_{x0} = 4\,\text{m}$, $\beta_{z0} = 11.5\,\text{m}$.

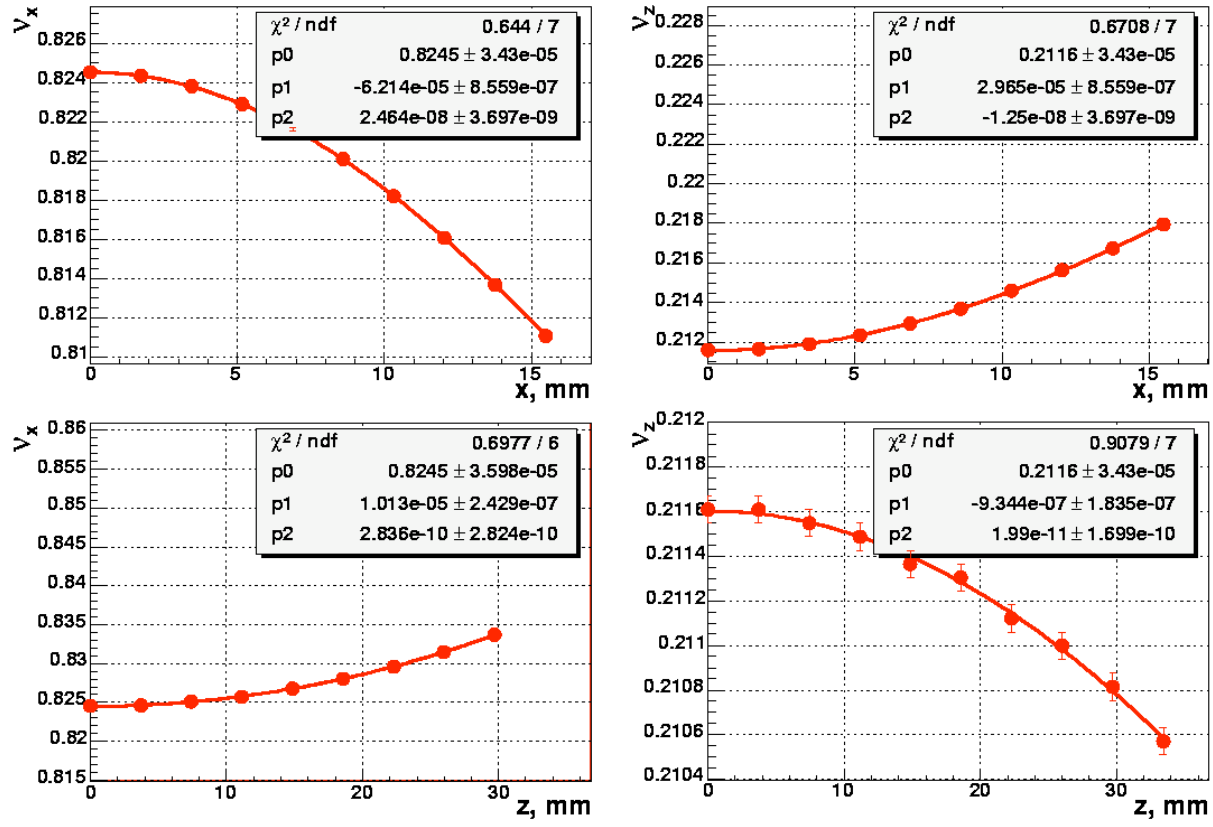

Figure 8: Tune deviation with the betatron oscillation amplitude.

Stochastic way of the DA limitation by uncontrollable interaction of high order resonances makes ineffective attempts to open the DA by main resonant harmonics optimization.

Another important characteristic of nonlinear motion is the dependence of the betatron tune on amplitude which is presented in Fig. 8. The dependence is not too strong: the largest tune shift at the border of the stable motion area is $\Delta Q_x(A_x^2) = -0.012$.

4 OFF-ENERGY DYNAMIC APERTURE

The simulations were done with two RF systems: the first, which is natural for DAΦNE (250 kV at 368 MHz for 510 MeV) compensates the radiation loss and the second at 1.3 GHz with a maximum voltage up to 10 MV providing the bunch compression. The high frequency cavity was inserted in the lattice as a point-like element at the FINUDA detector position.

Figure 9 shows the dynamic aperture reduction due to the synchrotron oscillation for different momentum deviations.

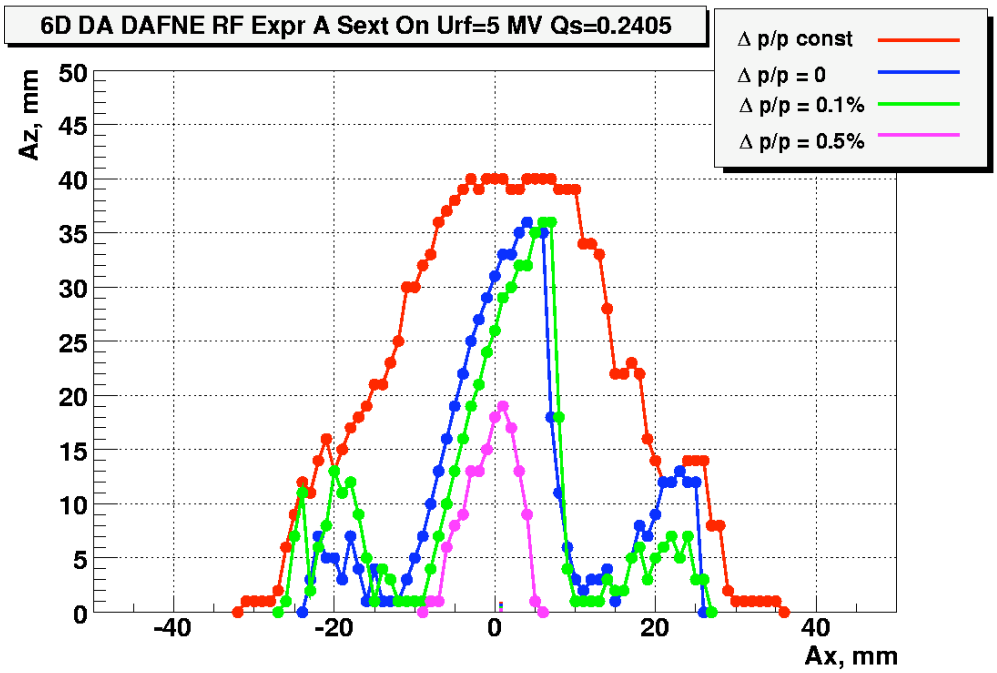

Figure 9: Dynamic aperture for 5 MV RF voltage. Red line corresponds to the on-energy case.

The off-energy DA shrinks significantly even for initial condition $\Delta p/p_0 = 0$ because due to the orbit elongation (synchro-betatron coupling) actual momentum deviation for $x(0) \approx 30\,\text{mm}$ is equal to $\Delta p/p_0 \sim 10^{-4}$ which is enough to activate synchrobetatron resonances (see also off-energy tune scans below).

Figure 10 shows the maximum transverse DA as a function of the synchrotron tune, which was varied by increasing of the 1.3 GHz voltage for several levels of momentum deviation.

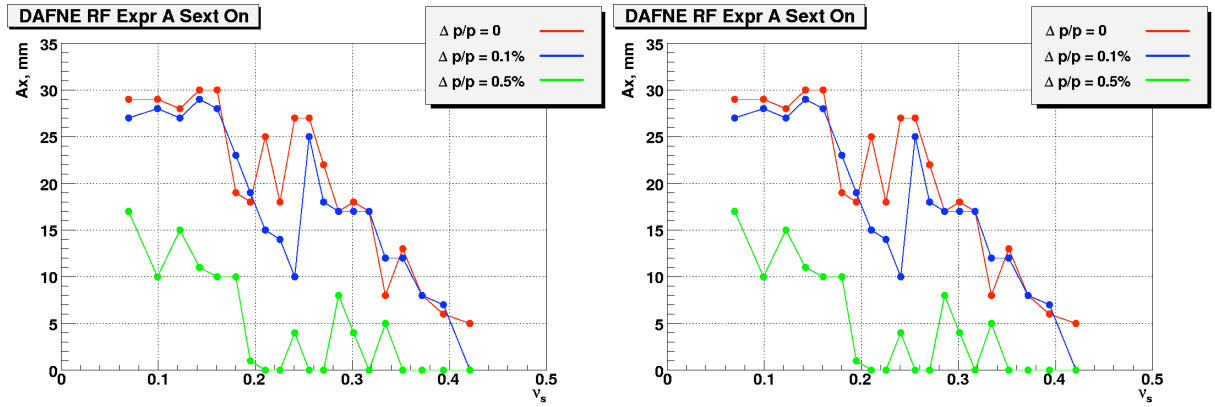

Figure 10: Transverse dynamic aperture vs. synchrotron tune. Synchrotron resonances effect (for instance at $Q_s = 0.25$) is clearly seen.

Figure 11 shows the maximum transverse dynamic aperture as a function of the momentum deviation.

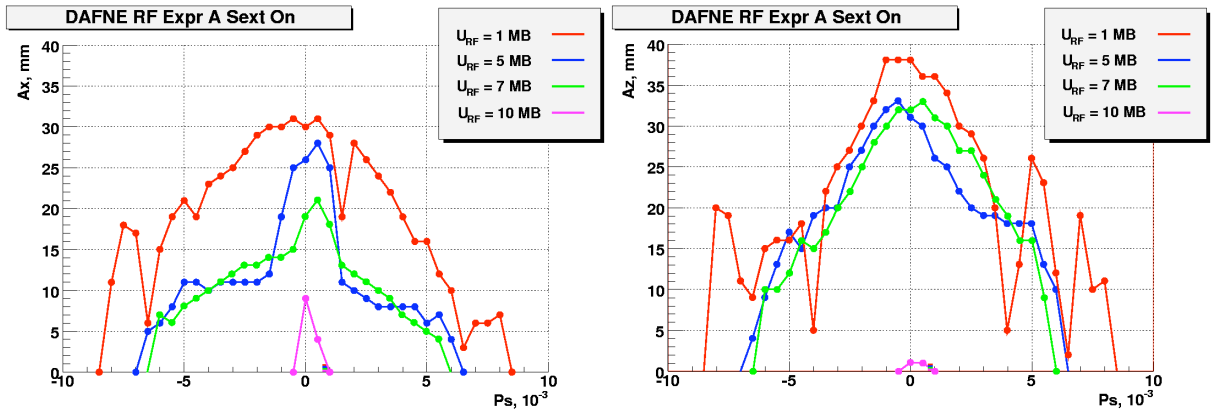

Figure 11: Transverse dynamic aperture vs. momentum deviation ($\sigma_e = 3.8 \times 10^{-4}$).

Figure 12 demonstrates the maximum energy dynamic aperture along the beam orbit. This dependence is responsible for the Touschek beam lifetime [5]. When the 1.3 GHz RF system is switched-off ($U_{RF} = 0$) the energy aperture is defined by the RF separatrix and is the constant with the azimuth. With the RF voltage increasing, the synchro-betatron coupling effects influence the energy dynamic aperture providing its modulation along the beam orbit together with the bunch length modulation. Fig.13 illustrates this process and shows the longitudinal phase space trajectories for different amplitudes of the 1.3 GHz RF voltage: U_{RF} =0, 1, 5 and 10 MV. For 1 MV one can see a distortion of the original RF potential well (the harmonic number ratio for 368 MHz and 1.3 GHz is 120/420) while for 5 MV and 10 MV the longitudinal phase space is determined completely by the high frequency system and the bunch compression is observed easily. The energy dynamic aperture for two last cases is also defined by the synchro-betatron coupling effect instead of RF bucket size as it is seen from the zoomed phase space curves.

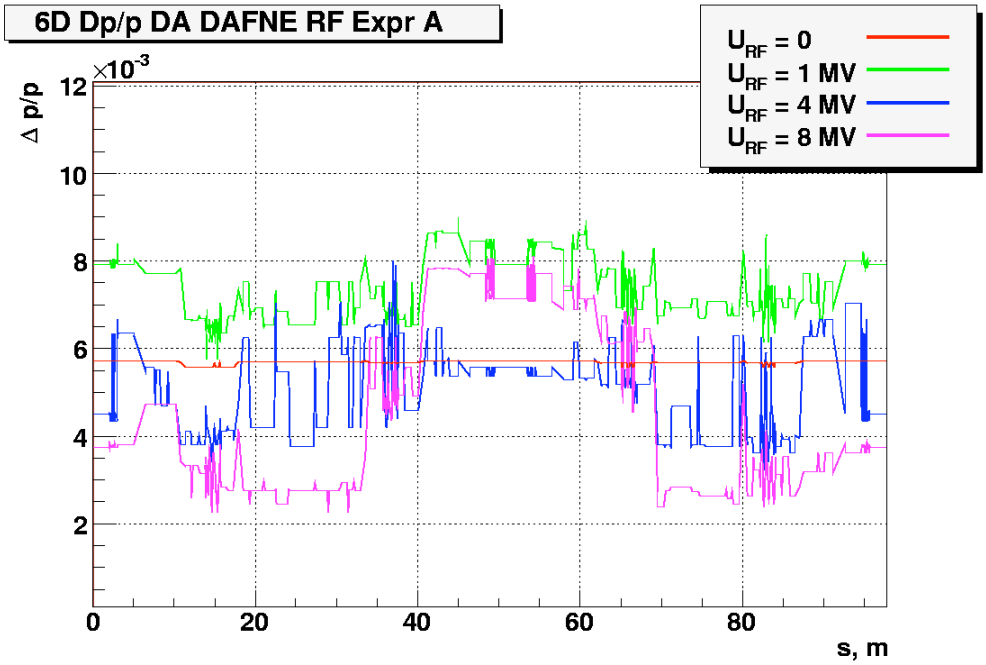

Figure 12: Energy dynamic aperture along the ring ($\sigma_e = 3.8 \times 10^{-4}$).

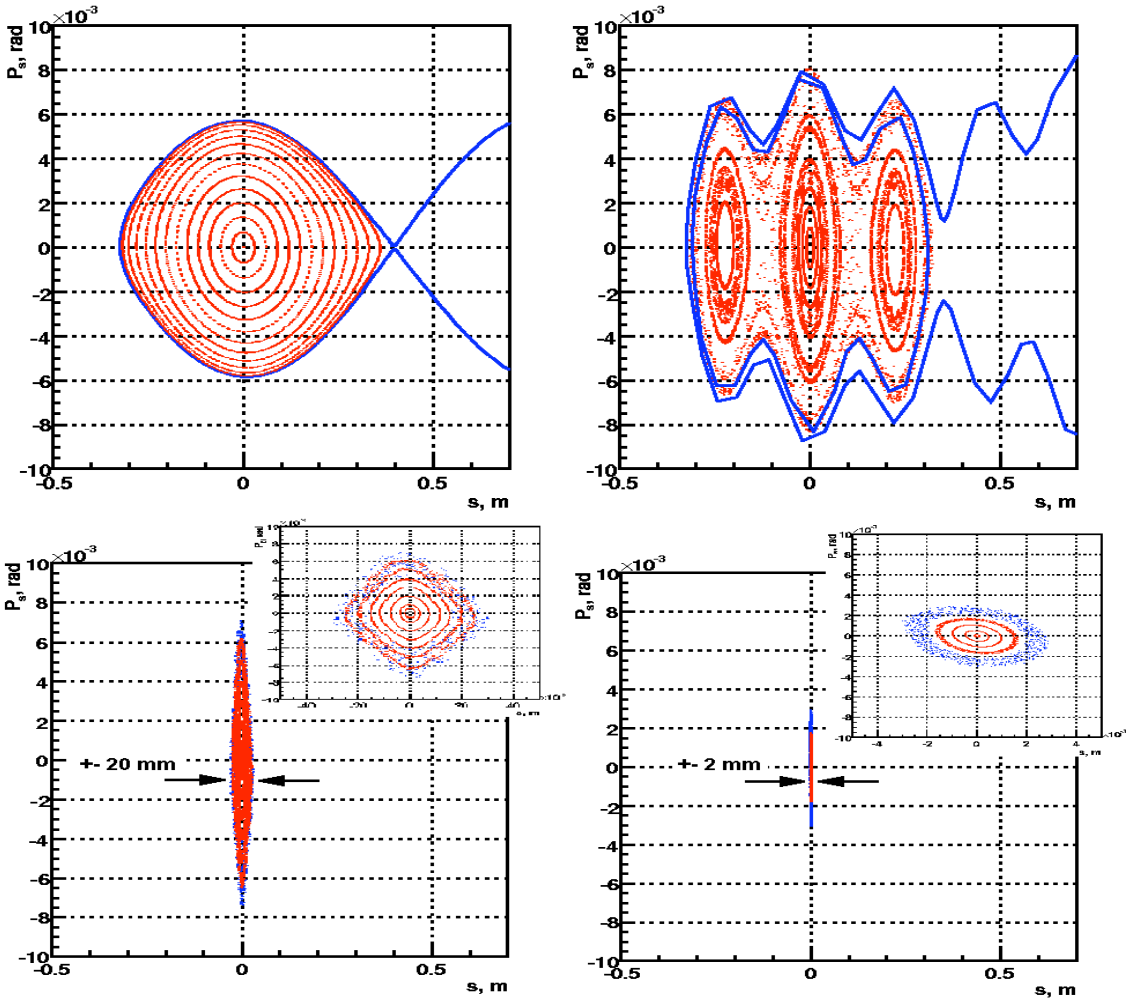

Figure 13: Longitudinal phase space trajectories. U_{RF} is the 1.3 GHz voltage.

5 TUNE SCAN AND TUNE POINT OPTIMIZATION

In the case under consideration, two sources of synchrobetatron coupling can be supposed. The first is the horizontal dispersion $D_x(s)$ in the strong chromatic sextupole magnets. Using the formalism of A.Piwinski we can estimate the effect. According to [6], the following main satellite resonances are excited by the horizontal dispersion in sextupole magnets:

Resonance	*Resonance width*
$2Q_x \pm Q_s = n$	$\Delta Q_x = \pm\hat{\delta}\left\lvert\sum_k\left[(ml)\cdot D_x\cdot\beta_x\cdot e^{2i\psi_x}\right]_k\right\rvert$
$2Q_z \pm Q_s = n$	$\Delta Q_z = \pm\hat{\delta}\left\lvert\sum_k\left[(ml)\cdot D_x\cdot\beta_z\cdot e^{2i\psi_z}\right]_k\right\rvert$
$Q_x \pm 2Q_s = n$	$\Delta Q_x = \pm\frac{\hat{\delta}^2}{2\sqrt{\varepsilon_x}}\left\lvert\sum_k\left[(ml)\cdot D_x^2\cdot\sqrt{\beta_x}\cdot e^{i\psi_x}\right]_k\right\rvert$

where $\hat{\delta}$ is the synchrotron oscillation amplitude: $\delta = \hat{\delta}\cdot\cos Q_s\theta$, $\varepsilon_x = A_x^2/\beta_{x0}$ and the sum is taken over sextupole magnets with integrated strength $(ml)_k$. Note, that only the rise times (inversely proportional to the resonance width) on $2Q_{x,z} \pm Q_s = n$ give an exponential increase. The rise time for $Q_x \pm 2Q_s = n$ depend on the horizontal amplitude and change with its variation.

The estimated width of the synchrobetatron resonances caused by the horizontal dispersion in the sextupoles is listed in Table 3 for $\hat{\delta} = 0.25\% \approx 6\sigma_e$ and $A_x = 5$ mm.

Table 3: Synchro-betatron satellites width.

Resonance	*Width*
$2Q_x \pm Q_s = n$	$\pm 5\times10^{-3}$
$2Q_z \pm Q_s = n$	$\pm 3\times10^{-3}$
$Q_x \pm 2Q_s = n$	$\pm 8\times10^{-3}$

All these satellites can be compensated by varying the sextupole strength so that the lattice factors for main resonances vanish.

The second possible source of coupling is linked to time variation of the betatron tunes, due to the simultaneous presence of momentum oscillations and finite chromaticity, which is our case but only for the vertical motion. So we can expect that this mechanism will produce satellites for the vertical and coupling betatron resonances:

$$m_x Q_x + \left(m_z Q_z + m_s Q_s\right) = n.$$

The strength of the satellite [7] is proportional to the main resonance strength with the factor determined by Bessel function:

$$\propto J_{m_s}\left(m_z\frac{\xi_z\hat{\delta}}{Q_s}\right).$$

The satellite lines are presented in Fig.14 at the scan of the maximum horizontal, vertical and energy dynamic aperture.

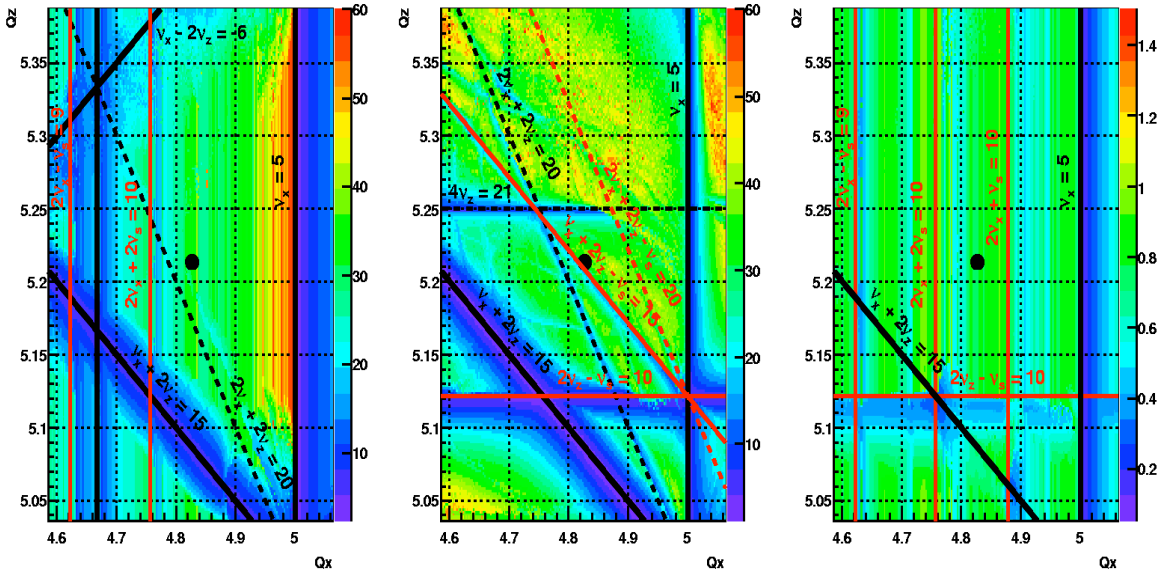

(a) Momentum oscillation amplitude $\hat{\delta} = 0$.

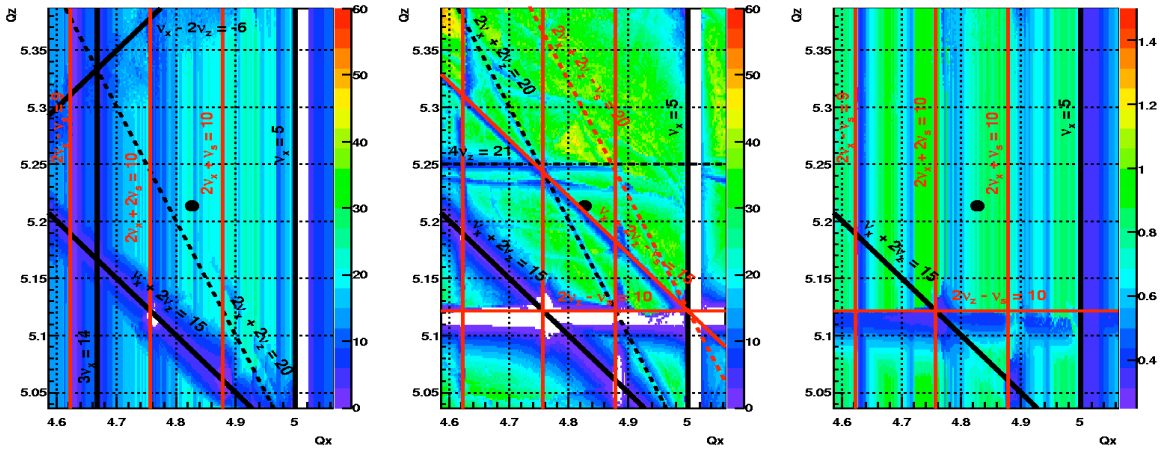

(b) Momentum oscillation amplitude $\hat{\delta} = 0.25\%$.

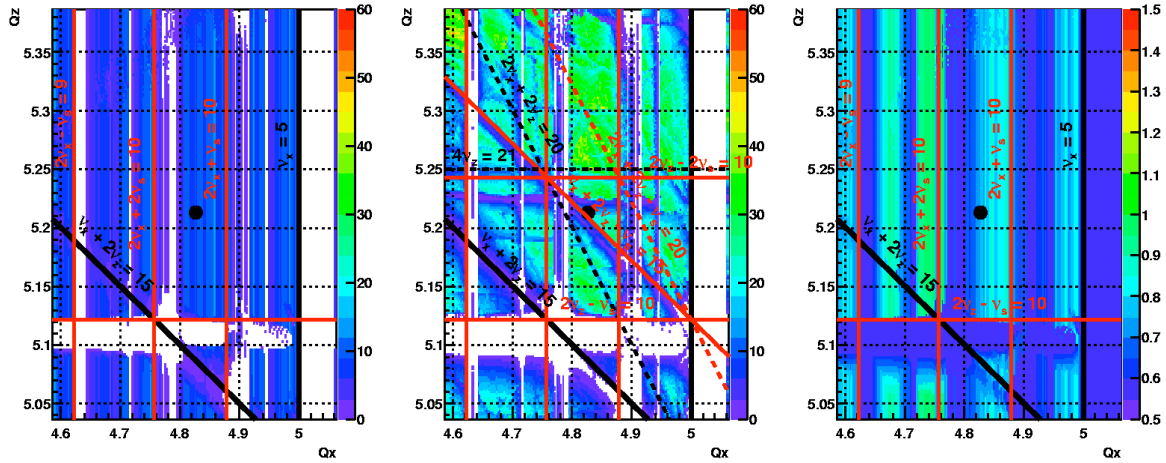

(c) Momentum oscillation amplitude $\hat{\delta} = 0.5\%$.

Figure 14: Off-energy dynamic aperture scan. The maximum achievable aperture is presented in mm for the transverse motion and $(\Delta p / p_0)_{\max}$ % for the longitudinal motion.

In Fig.14 black lines show main betatron resonances while red lines indicate synchrobetatron satellites.

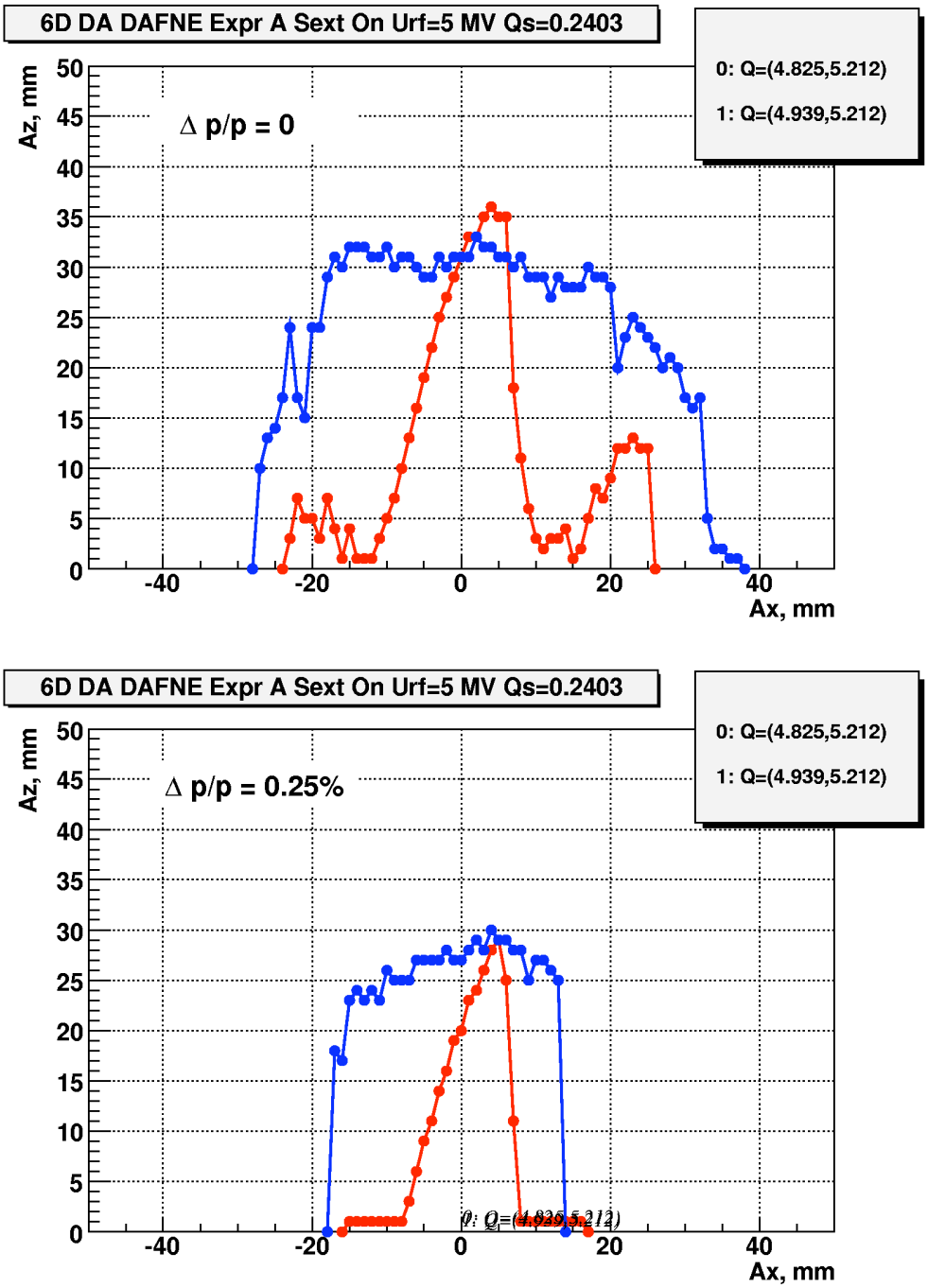

Figure 15: The dynamic aperture in the alternative working point (blue) compare to the initial tune point (red).

Dynamic aperture scans in Fig.14 allow finding a new working point for the SRFF DAΦNE experiment with higher value of dynamic aperture. A possible solution (4.939, 5.212) is demonstrated in Fig.15 where the dynamic aperture in the new working point is shown in comparison with the old one.

5 CONCLUSIONS

A simulation of the nonlinear beam dynamics and dynamic aperture has been performed for the DAΦNE storage ring in the strong RF focusing operation mode. The bunch length modulation in this mode gives the chance to reduce the vertical betatron function in the interaction point and hence to increase luminosity. Due to strong coupling of the transverse and longitudinal oscillations in this regime synchrobetatron resonances decrease the dynamic aperture in the chosen tune point drastically. However it is possible to find alternative working point by fine tune adjustment in such way to obtain the dynamic aperture which seems large enough.

Improvement in the vertical chromaticity compensation seems reasonable to reduce strength of the modulation synchrobetatron resonances. Searching of new sextupole arrangement that provides both natural chromaticity compensation and reduction of the synchrobetatron lattice factors might be promising to open the dynamic aperture.

6 REFERENCES

References in the bibliography must be referred to in the text by a superscript number with a right–hand parenthesis only. Put initials, last name of the author(s), volume (bold face), page number, year (in brackets) of publication. Spacing Exacly 14pt. Example:

[1] A. Gallo, P. Raimondi, M. Zobov, "The Strong RF Focusing: a Possible Approach to Get Short Bunches at the IP", e-Print Archive: physics/0404020. Proceedings of the 31th ICFA Beam Dynamics workshop, SLAC 2003. C. Biscari, Bunch length modulation in highly dispersive storage rings, http://link.aps.org/abstract/PRSTAB/v8/e091001.

[2] D. Alesini et al., "Proposal of a bunch length modulation experiment in DAΦNE", LNF-05/04(IR), 22-Feb-2005.

[3] P. Piminov. Master's thesis, BINP, Novosibirsk, 2000 (in Russian).

[4] G. Ripken – DESY Report 85-084, August 1985.

[5] E. Levichev, S.Nikitin, P.Piminov , "Simulation of Touschek effect for DAΦNE with strong RF focusing", ICFA Mini-Workshop on "Frontiers of Short Bunches in Storage Rings", INFN-LNF, Frascati, 7-8 November 2005.

[6] A. Piwinski, "Synchrotron Sidebands of Betatron Coupling Resonances", DESY 93-189 (1993).

[7] G. Guignard, "Hamiltonian treatment of synchrobetatron resonances", CERN SL/94-09 (AP).